BIOCHEMISTRY
including biophysical chemistry & molecular biology

Article

pubs.acs.org/biochemistry

Membrane Depth-Dependent Energetic Contribution of the Tryptophan Side Chain to the Stability of Integral Membrane Proteins

Heedeok Hong,*[,†] Dennis Rinehart,[‡] and Lukas K. Tamm*[,‡]

[†]Department of Chemistry and Department of Biochemistry and Molecular Biology, Michigan State University, East Lansing, Michigan 48824, United States

[‡]Center for Membrane Biology and Department of Molecular Physiology and Biological Physics, University of Virginia, Charlottesville, Virginia 22908, United States

Supporting Information

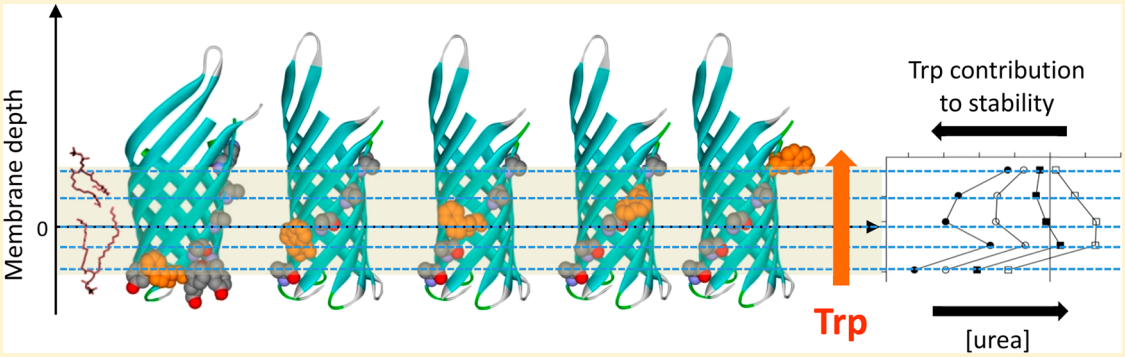

ABSTRACT: Lipid solvation provides the primary driving force for the insertion and folding of integral membrane proteins. Although the structure of the lipid bilayer is often simplified as a central hydrophobic core sandwiched between two hydrophilic interfacial regions, the complexity of the liquid-crystalline bilayer structure and the gradient of water molecules across the bilayer fine-tune the energetic contributions of individual amino acid residues to the stability of membrane proteins at different depths of the bilayer. The tryptophan side chain is particularly interesting because despite its widely recognized role in anchoring membrane proteins in lipid bilayers, there is little consensus about its hydrophobicity among various experimentally determined hydrophobicity scales. Here we investigated how lipid-facing tryptophan residues located at different depths in the bilayer contribute to the stability of integral membrane proteins using outer membrane protein A (OmpA) as a model. We replaced all lipid-contacting residues of the first transmembrane β-strand of OmpA with alanines and individually incorporated tryptophans in these positions along the strand. By measuring the thermodynamic stability of these proteins, we found that OmpA is slightly more stable when tryptophans are placed in the center of the bilayer and that it is somewhat destabilized as tryptophans approach the interfacial region. However, this trend may be partially reversed when a moderate concentration of urea rather than water is taken as the reference state. The measured stability profiles are driven by similar profiles of the *m*-value, a parameter that reflects the shielding of hydrophobic surface area from water. Our results indicate that knowledge of the free energy level of the protein's unfolded reference state is important for quantitatively assessing the stability of membrane proteins, which may explain differences in observed profiles between *in vivo* and *in vitro* scales.

The thermodynamic stability of polytopic membrane proteins is determined by a delicate balance between lipid solvation and packing of amino acid side chains within cell membranes.[1,2] Favorable transfer of side chains into the hydrophobic core of a lipid bilayer is crucial for the topological localization and stabilization of membrane proteins. Thus, hydrophobicity scales, which represent quantitative measures of individual side chains to partition between water and hydrophobic environments, are powerful tools not only for identifying the membrane-spanning polypeptide segments but also for predicting the stability of membrane proteins.[3]

Among the many existing hydrophobicity scales, four experimentally determined scales are particularly useful for understanding the contribution of lipid solvation to the thermodynamic stability of membrane proteins: the Wimley–White whole-residue scales based on water–octanol and water–membrane interface partitioning of model pentapeptides,[4,5] the Hessa–von Heijne scale based on translocon–endoplasmic reticulum (ER) membrane partitioning of model

Received: March 16, 2013
Revised: April 29, 2013
Published: May 29, 2013

transmembrane segments,[6,7] and the Moon–Fleming scale based on the folding equilibrium of β-barrel membrane protein OmpLA between water and the lipid bilayer.[8] In these scales, unique transfer free energy values were determined for each amino acid side chain using an organic solvent, the membrane interface, or the center of the hydrophobic core of a bilayer as the reference hydrophobic environment.

However, the latter two studies also showed that the transfer free energies of amino acid side chains strongly depend on the depth at which the side chain is embedded in the bilayer.[7,8] Computational and statistical analyses of the structures of membrane proteins revealed a strong positional dependence of side chain distributions along the bilayer normal.[7,9−11] These findings suggest that the complexity of the liquid-crystalline bilayer structure adjusts the energetic contribution of individual side chains to membrane protein stability at different depths. However, it is still not clear for most side chains how this depth dependence is related to the thermodynamic stability of membrane proteins.

Here, we determined the energetic contribution of the tryptophan (Trp) side chain to the thermodynamic stability of β-barrel outer membrane protein A (OmpA) at different depths in a fluid lipid bilayer. Tryptophan is particularly interesting because it is known to play an important role in anchoring membrane proteins in lipid bilayers.[12−15] Although there is considerable consensus among the different hydrophobicity scales at least on the qualitative hydrophobic ranking of most side chains, there is a surprisingly wide range of values found for the hydrophobicity of Trp. On the Nozaki–Tanford[16] and Wimely–White octanol and interface scales, Trp is the most hydrophobic residue, but it is only moderately hydrophobic on the Kyte–Doolittle,[17] Eisenberg–Weiss,[18] Engelman–Steiz–Goldman,[19] Hessa–von Heijne,[6] and Moon–Fleming[8] scales. One possibility, which we are exploring here, is that Trp's contribution to the stability of membrane proteins is particularly dependent on membrane depth and its context in the protein sequence. An improved knowledge of factors that contribute to this stability is therefore crucial for understanding Trp's role in membrane protein folding.

It has been recognized by several groups that the folding of β-barrel membrane proteins can be used as a powerful model system to study the energetics of lipid–protein interactions. In a few cases, including OmpA, β-barrel membrane proteins have been shown to reversibly unfold in urea or guanidinium solutions from their folded state in lipid bilayers.[8,20,21] Thus, via mutation of the lipid-contacting residues, the contribution of lipid solvation of specific residues to the thermodynamic stability of membrane proteins can be estimated.[8,22] In this work, we replaced all lipid-contacting residues of the first β-strand of OmpA with alanines (Ala) and individually incorporated tryptophans at these positions along the strand. By measuring the thermodynamic stability of these proteins, we found that OmpA is slightly more stable when Trp is placed in the center of the lipid bilayer and that it is somewhat destabilized as Trp approaches the interfacial regions of the bilayer. However, interfacial tryptophans may be more stabilizing than central tryptophans when 3 M urea rather than buffered water is taken as the reference state, i.e., a condition that may better reflect folding conditions *in vivo*.

MATERIALS AND METHODS

DNA Construct. All site-directed mutagenesis was conducted by using the QuickChange kit (Agilent). First, the quadruple mutant W7A/T9A/L13A/W15A of full-length mature OmpA was generated and named W_0. Plasmid pET1113 encoding the wild-type *proOmpA* gene was used as a template.[23] Next, using W_0 as a new template, Ala7, Ala9, Ala11, Ala13, and Ala15 were individually mutated to tryptophans to generate W_7, W_9, W_{11}, W_{13}, and W_{15}, respectively. The *Escherichia coli* BL21(DE3) (Δ*lamB ompF::Tn5* Δ*ompA* Δ*ompC*)[24] cells were transformed with the mutant plasmids for expression of OmpA. In this *E. coli* strain, chromosomally encoded OmpA and all other major outer membrane porin genes were deleted so that mutant OmpA could be purified without any interference from intrinsic wild-type OmpA.

Expression and Purification of OmpA. The detailed procedure for the expression and purification of OmpA was described previously.[22] Briefly, 20 mL of transformed *E. coli* cells grown overnight was inoculated in 1 L of LB medium containing 0.1 g/L ampicillin and cultured at 37 °C. The expression of OmpA was induced by addition of 1 mM IPTG (isopropyl β-D-1-thiogalactopyranoside) when OD_{600} reached approximately 0.6. The cells were grown for an additional 4–5 h and harvested. The wet cell paste was resuspended in 15 mL of solution A {0.75 M sucrose, 10 mM Tris-HCl [tris(hydroxymethyl)aminomethane hydrochloride] (pH 5.0), and 0.05% β-mercaptoethanol (v/v)} per liter of culture. Solution B [10 mL/L of culture; 40 mM EDTA (ethylenedinitrilotetraacetic acid), 10 mM Tris-HCl (pH 7.0), 50 μg/mL lysozyme, and 0.05% β-mercaptoethanol] was then added while the mixture was being stirred and cooled in ice for 1 h. After the concentration of β-mercaptoethanol had been increased to 0.2%, the resuspension was French-pressed twice. Solid urea (Sigma, SigmaUltra grade) was sequentially added to the stirred lysate at room temperature until the final concentration reached 4 M. Titanium dust and cell debris were removed by centrifugation at 2000*g* (4 °C for 30 min). The supernatant was ultracentrifuged at 32000 rpm (4 °C for a minimum of 6 h) in a 45 Ti rotor (Beckman-Coulter) to spin down the pre-extracted total membrane fraction.

The pre-extracted membranes were resuspended in 10 mL of an 8 M urea solution/L of culture (SigmaUltra grade) containing 20 mM Tris-HCl (pH 8.0) and 0.1% β-mercaptoethanol by the use of a Potter homogenizer at room temperature. A nominal 10 mL of pure 2-propanol was added to the resuspension in a glass vial, and the whole mixture was incubated at 55 °C in a preheated water bath for exactly 30 min. This step is critical for the extraction of OmpA from the outer membrane. After the extraction, the sample was rapidly cooled in ice until a temperature of <10 °C was reached. The mixture was ultracentrifuged at 28000 rpm and 4 °C for at least 90 min in a 45 Ti rotor. The unfolded OmpA solubilized in the supernatant was further purified by anion-exchange column chromatography (25 mL Q-Sepharose, fast flow, GE Healthcare) using a fast protein liquid chromatography system (Bio-Rad). The column was equilibrated with 2-propanol mixed with an equal volume of buffer [15 mM Tris-HCl (pH 8.5), 0.1% β-mercaptoethanol, and 8 M urea (reagent grade, Sigma)]. After the sterile-filtered sample had been loaded, the protein-bound column was washed with a buffer solution containing 15 mM Tris-HCl (pH 8.5), 0.05% β-mercaptoethanol, and 8 M urea. Then, OmpA was eluted by a linear salt gradient from 0 to 100 mM NaCl [15 mM Tris-HCl (pH 8.5), 0.05% β-mercaptoethanol, and 8 M urea]. Combined fractions of high-purity OmpA were concentrated in a stirred ultrafiltration cell

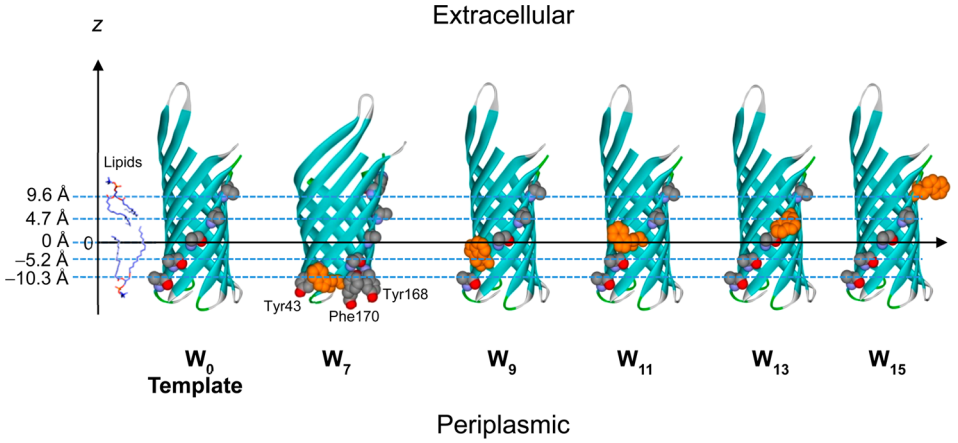

Figure 1. Scheme for Trp scanning to study the effect of tryptophans at different membrane depths on the thermodynamic stability of OmpA. The template mutant W_0 with all alanines in the β1 strand of the OmpA structure (Protein Data Bank entry 1QJP) is shown at the left. Single tryptophans (orange) are alternately substituted at positions 7 (W_7), 9 (W_9), 11 (W_{11}), 13 (W_{13}), and 15 (W_{15}) of β1. Tyr43 in strand β2 and Tyr168 and Phe170 in strand β8, which may participate in aromatic interactions with Trp, are highlighted in the W_7 mutant. The distances of the C_α positions of the lipid-contacting residues in β1 from the virtual central plane of a bilayer as obtained from the PDB-TM database[28] are shown on the *z*-axis.

(Amicon; 10 kDa cutoff filter) to a final concentration of 20–50 mg/mL as estimated by the Bradford protein assay (Bio-Rad).

Small Unilamellar Vesicles. Stock solutions of 1,2-dipalmitoleoyl-*sn*-glycero-3-phosphocholine (DPoPC) (Avanti Polar Lipids) and 1-palmitoyl-2-oleoyl-*sn*-glycero-3-[phospho-*rac*-(1-glycerol)] (POPG) (Avanti Polar Lipids) dissolved in chloroform were mixed to a molar ratio of 9:1 (DPoPC:-POPG). A total of 12 μmol of lipid was dried under a stream of nitrogen gas and further in a high-vacuum desiccator for 2 h. The dried lipid was thoroughly mixed with 1.2 mL of 10 mM glycine buffer (pH 9.2 and 1.0 mM EDTA) to yield a final lipid concentration of 10 mM. The lipid dispersion was sonicated for 50 min in an ice–water bath using a Branson ultrasonifier microtip at 50% duty cycle. Titanium dust was removed by centrifugation at 8000 rpm for 15 min twice, and the resulting SUVs were equilibrated overnight at 4 °C.

Refolding and Urea-Induced Equilibrium Unfolding of OmpA. Concentrated OmpA unfolded in 8 M urea was diluted 50–100-fold in 10 mM SUVs to a final protein concentration of 12 μM. The refolding reaction mixture was incubated for 3 h at 37 °C. Minor residues of aggregated protein formed during refolding were removed by centrifugation at 6000 rpm for 10 min twice. Refolded OmpA–lipid complexes were further diluted in aliquots at different urea concentrations in 10 mM glycine buffer [1 mM EDTA (pH 9.2)]. The dilution was 10-fold for fluorescence and 2.5-fold for SDS–PAGE experiments. The unfolding reaction mixtures were incubated with the desired concentrations of urea at 37 °C overnight to reach equilibrium.

Fluorescence Spectroscopy. Fluorescence spectra were recorded in a Fluorolog-3 spectrofluorometer (Horiba). The excitation wavelength was 290 nm, and the Trp fluorescence of OmpA at different urea concentrations was measured over the range of 300–400 nm; 4.2 nm slits were used for both excitation and emission. All spectra were background-subtracted with a proper reference sample with an identical composition but without protein.

SDS–PAGE Shift Assay. The equilibrated samples were mixed with the same volume of SDS sample buffer. The mixtures were loaded on 12.5% SDS–PAGE without heating.

Fitting of Equilibrium Unfolding Curves. The fitting procedures for obtaining the free energy of unfolding of OmpA were essentially the same as the procedure previously described by Hong and Tamm[20] but described in more detail in the Supporting Information. Fluorescence spectra were parametrized by calculating an average emission wavelength, $\langle\lambda\rangle$, defined as $\langle\lambda\rangle = \sum(F_i\lambda_i)/\sum F_i$. λ_i and F_i are the wavelength and the corresponding fluorescence intensity, respectively, at the *i*th measuring step in the spectrum. The unfolding curves, $\langle\lambda\rangle$ versus [urea], were fit to the following form of the two-state model using IgoPro (Wavemetrics).[20]

$$\langle\lambda\rangle = \frac{\langle\lambda\rangle_F + \langle\lambda\rangle_U \frac{1}{Q_R}\exp\left[\frac{m([\text{urea}]-C_m)}{RT}\right]}{1 + \frac{1}{Q_R}\exp\left[\frac{m([\text{urea}]-C_m)}{RT}\right]} \quad (1)$$

where $\langle\lambda\rangle_F$ and $\langle\lambda\rangle_U$ are the average emission wavelengths of the folded and unfolded states, respectively, determined from linear extrapolations to 0 M urea of the plateau values of the two states, C_m is the urea concentration at which the fractions of folded and unfolded states are equal, and Q_R is the relative ratio of the total fluorescence intensity of the native state to that of the unfolded state and is needed for normalization when one uses $\langle\lambda\rangle$ values to represent species concentrations. The unfolding free energy was obtained from the fitted values of C_m and m[25]

$$\Delta G^\circ_{\text{unfold},H_2O} = mC_m \quad (2)$$

The contribution of the lipid-contacting Trp residues to the stability of OmpA was calculated at different membrane depths:

$$\Delta\Delta G^\circ_{\text{Trp-Ala}} = \Delta G^\circ_{\text{unfold},W_0}([\text{urea}]) - \Delta G^o_{\text{unfold},W_x}([\text{urea}]) \quad (3)$$

where $\Delta G^\circ_{\text{unfold},W_0}([\text{urea}])$ is the unfolding free energy of the W_0 mutant with no Trp in the β1 strand at a specific urea concentration and $\Delta G^\circ_{\text{unfold},W_x}([\text{urea}])$ corresponds to the unfolding free energy of W_x, in which *x* designates the position of the Trp in β1.

The unfolding free energy of a protein $[\Delta G^\circ_{\text{unfold},W_x}([\text{urea}])]$ at a certain urea concentration was obtained from

dx.doi.org/10.1021/bi400344b | *Biochemistry* 2013, 52, 4413–4421

$$\Delta G^{\circ}_{unfold}([urea]) = \Delta G^{\circ}_{unfold,H_2O} - m[urea] = m(C_m - [urea]) \quad (4)$$

where $\Delta G^{\circ}_{unfold,H_2O}$ is the unfolding free energy at 0 M urea, which is obtained from eq 2. The statistical significance of the differences in $\Delta\Delta G^{\circ}_{Trp\text{-}Ala}$ (Figure 4) was evaluated by an ANOVA test.[26] Each data set included the $\Delta\Delta G^{\circ}_{Trp\text{-}Ala}$ and the upper and lower standard error limits of $\Delta\Delta G^{\circ}_{Trp\text{-}Ala}$ for each mutant.

RESULTS

Strategy for Measuring the Depth-Dependent Contribution of Trp to the Stability of Membrane Proteins. To study the energetics of the lipid solvation of Trp side chains in the context of a native membrane protein structure, it is important to maximize the exposure of Trp to the surrounding lipids while minimizing its interactions with neighboring side chains. Thus, we chose the first transmembrane β-strand (β1) and replaced all lipid-contacting residues with the small nonpolar side chain Ala (Figure 1, template). Choosing β1 for this purpose had two advantages. First, β1 has fewer aromatic residues in the neighboring β2 and β8 than any other strand. This is important because we have previously shown that some tryptophans can favorably interact with other closely located aromatic residues and thereby enhance the protein's stability, while simultaneously reducing the maximal level of lipid solvation of the side chain.[22] β2 and β8 harbor only three aromatic residues, i.e., Tyr43 (β2), Tyr168 (β8), and Phe170 (β8), which are all located in the periplasmic interface region of the membrane.[27] The other lipid-contacting residues in β2 (Leu35, Ala37, Ala39, and Gly41) and β8 (Leu162, Leu164, and Val166) are mostly composed of small- and moderate-sized nonpolar side chains. Therefore, Trp7 is the only Trp in β1 that may interact with those nearby aromatic residues. The second reason for choosing β1 for mutagenesis was that the number of required point mutations was small compared to the number in other strands and two of the tested Trp positions were native tryptophans, which we reasoned would only slightly perturb the correct folding of the mutant protein. The lipid-contacting residues in β1 are Trp7, Thr9, Ala11, Leu13, and Trp15. Thus, quadruple mutant W7A/T9A/L13A/W15A converted all lipid-facing residues of β1 to Ala. The resulting OmpA mutant (also termed W_0) served as a template for all Trp scanning mutations of this work. On the basis of this template, a series of OmpA Trp mutants termed W_7, W_9, W_{11}, W_{13}, and W_{15} were generated as depicted in Figure 1.

To estimate the distances of individual Trp side chains from the membrane center, we used the PDB-TM database (http://pdbtm.enzim.hu) and applied it to the crystal structure of OmpA.[28] According to this analysis, the central plane of the lipid bilayer passes through OmpA very close to the C_α position of residue 11 (Figure 1). The distances of the C_α atoms of residues 7, 9, 11, 13, and 15 from the bilayer center are listed in Table 1.

Folding Efficiency of OmpA Mutants with Tryptophans at Different Membrane Depths. First, we tested the refolding efficiency of the template and the five single β1 Trp mutants of OmpA in small unilamellar vesicles (SUVs) composed of DPoPC and POPG (9:1) using the SDS–PAGE shift assay. Without sample heating, correctly folded and membrane-inserted full-length OmpA migrates as a 30 kDa form while surface-adsorbed or unfolded proteins migrate as 35 kDa forms on SDS–PAGE gels.[29,30] As shown in Figure S1A of the Supporting Information, refolding was generally efficient for all mutants, with yields varying from 87 to 98% . Tryptophan fluorescence spectra of refolded mutants in SUVs were also similar to each other, with the maximal emission wavelengths ranging between 334 and 336 nm (Figure S1B of the Supporting Information), clearly different from the emission maxima of the respective unfolded proteins (Figure S1C of the Supporting Information). These observations indicate that the rather invasive quadruple mutations were tolerated by the robust folding and membrane-insertion capability of OmpA. A calculation of the difference free energy changes of water-to-membrane transfer of the four mutations using the Wimley–White water–octanol scale for core residues 9 and 13 ($\Delta\Delta G^{\circ}_{Thr9\text{-}Ala9}$ and $\Delta\Delta G^{\circ}_{Leu13\text{-}Ala13}$, respectively) and the water–interface scale for interfacial residues 7 and 15 ($\Delta\Delta G^{\circ}_{Trp7\text{-}Ala7}$ and $\Delta\Delta G^{\circ}_{Trp15\text{-}Ala15}$, respectively) showed that the sum or energy penalty for all four mutations ($\Delta\Delta G^{\circ}$) is 6.5 kcal/mol.[4,5] Because the stability of wild-type OmpA in DPoPC/POPG bilayers ($\Delta G^{\circ}_{fold,H_2O}$) is −9.2 kcal/mol,[22] one might expect that membrane insertion of quadruple mutant W_0 would still be favorable by approximately −3 kcal/mol. Interestingly, the experimental thermodynamic stability of mutant W_0 ($\Delta G^{\circ}_{fold,H_2O}$) was −2.5 kcal/mol (see Table 1), i.e., 6.7 kcal/mol less stable than the wild type, which is close to the Wimley–White scale-based prediction. Unfolding was also efficient (80–100%) for most mutants, but somewhat less efficient for W_0 and W_9 (~70%) as judged by the SDS–PAGE assay (Figure S1A of the Supporting Information). We do not completely understand the impaired unfolding efficiency of some of the mutants, but this does not affect the subsequent fluorescence-based analysis, which considers only the fraction that does unfold.

Table 1. Fitted Parameters of Urea-Induced Equilibrium Unfolding of OmpA Monitored by Tryptophan Fluorescence

	C_α–bilayer center distance (Å)	C_m (M)	m (kcal mol^{-1} M^{-1})	$\Delta G^{\circ}_{unfold,H_2O}$ (kcal/mol)
W_0	none	2.0 ± 0.1	1.2 ± 0.1	2.5 ± 0.2
W_7	−10.3	3.0 ± 0.1	2.1 ± 0.2	6.3 ± 0.5
W_9	−5.2	1.9 ± 0.1	2.2 ± 0.1	4.2 ± 0.4
W_{11}	0	2.1 ± 0.1	2.7 ± 0.3	5.4 ± 0.7
W_{13}	4.7	2.2 ± 0.1	2.3 ± 0.2	5.1 ± 0.5
W_{15}	9.6	2.2 ± 0.1	1.7 ± 0.1	3.7 ± 0.4

Equilibrium Unfolding of OmpA Mutants. The thermodynamic stabilities of the OmpA mutants were measured by urea-induced equilibrium unfolding monitored by Trp fluorescence in 9:1 DPoPC/POPG bilayers (Figure 2). Sigmoidal curves were observed for all mutants, and the linearization of unfolding free energy $\Delta G^{\circ}_{unfold}$ versus urea concentration according to the two-state model (see Materials and Methods) yielded straight lines with a slope of m and an intercept of $\Delta G^{\circ}_{unfold,H_2O}$. The fitted midpoints of unfolding transition C_m and the linear dependence of $\Delta G^{\circ}_{unfold}$ on urea concentration (m-value) are plotted against the Trp position along strand β1 in panels A and B of Figure 3. The product of C_m and m yields the unfolding free energy in water, $\Delta G^{\circ}_{unfold,H_2O}$ (eq 2),[25] which is plotted against the Trp position in Figure 3C. These best fit thermodynamic parameters are listed in Table 1 for each of the mutants.

dx.doi.org/10.1021/bi400344b | Biochemistry 2013, 52, 4413–4421

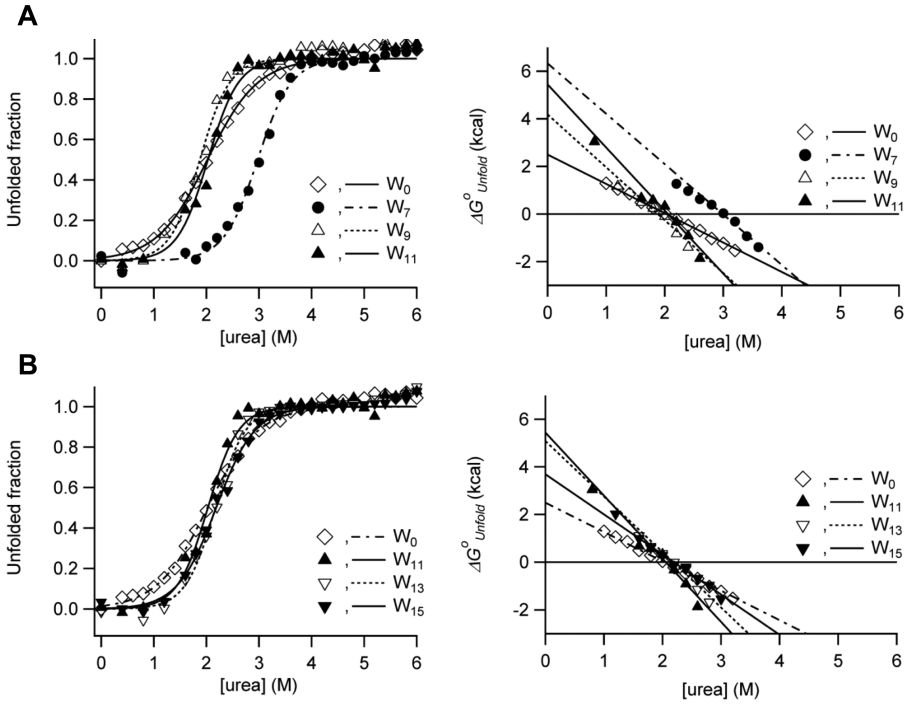

Figure 2. Urea-induced equilibrium unfolding of OmpA mutants in 9:1 DPoPC/POPG lipid bilayers monitored by Trp fluorescence emission. (A) Unfolding transition curves for W_0, W_7, W_9, and W_{11} mutants with tryptophans in the periplasm-facing monolayer (left) and corresponding plots of unfolding free energies vs urea concentration (right). (B) Unfolding transition curves for W_0, W_{11}, W_{13}, and W_{15} mutants with tryptophans in the extracellular space-facing monolayer (left) and corresponding plots of unfolding free energies vs urea concentration (right).

Among the mutants tested, W_0 with no lipid-contacting Trp in β1 showed the lowest C_m and m (2.0 M and 1.2 kcal mol^{-1} M^{-1}, respectively) and thus the lowest thermodynamic stability ($\Delta G^{\circ}_{unfold,H_2O}$ = 2.5 ± 0.2 kcal/mol). When a Trp residue was substituted at position 7, C_m increased significantly to 3.0 M. This mutant will be further discussed below. All other mutants had rather moderate shifts of C_m values, which were still comparable to the level of W_0 (Figure 3A). On the other hand, the m-values exhibited continuous changes generating a bell-shaped curve as a function of Trp position (Figure 3B). A maximal value of 2.7 kcal mol^{-1} M^{-1} was reached when Trp was placed near the center of the bilayer (W_{11} mutant), and the m-values gradually decreased (to 2.1 kcal mol^{-1} M^{-1} for W_7 and 1.7 kcal mol^{-1} M^{-1} for W_{15}) as Trp was moved toward both interfacial regions.

Membrane Depth-Dependent Contribution of Trp to the Stability of OmpA. The contribution of lipid solvation of tryptophans to the stability of OmpA was evaluated by calculating the difference unfolding free energy ($\Delta\Delta G^{\circ}_{Trp\text{-}Ala}[W_x] = \Delta G^{\circ}_{unfold}[W_0] - \Delta G^{\circ}_{unfold}[W_x]$, where x = 7, 9, 11, 13, or 15) between two mutants in the presence and absence of individual tryptophans in β1 (eqs 3 and 4 and Figure 4). Large negative values of $\Delta\Delta G^{\circ}_{Trp\text{-}Ala}[W_x]$ indicate favorable contributions of tryptophans to OmpA's thermodynamic stability and excellent solvation of these tryptophans by membrane lipids. In general, stabilization of OmpA by lipid-solvated tryptophans depended quite strongly on the membrane depth, structural context, and concentration of the denaturant urea. At 0 M urea, tryptophans in all lipid-contacting positions along β1 stabilized OmpA ($\Delta\Delta G^{\circ}_{Trp\text{-}Ala}[W_x] < 0$). OmpA was more stable when Trp was located near the center of the lipid bilayer (Trp11) and gradually became destabilized as Trp was moved toward both interfaces. For example, the central Trp11 was 1.8 ± 0.7 kcal/mol more stable than the interfacial Trp15 (Figure 4 and Table 1). An ANOVA test with the four $\Delta\Delta G^{\circ}_{Trp\text{-}Ala}$ values for W_9, W_{11}, W_{13}, and W_{15} mutants at 0 M urea yielded a p of 0.0042, which is below the p = 0.01 significance threshold and indicates that this trend is statistically significant. Apart from Trp7, the symmetric trend of $\Delta\Delta G^{\circ}_{Trp\text{-}Ala}$ around Trp11 further indicates that the difference in curvature between the inner and outer leaflets of SUVs appears not to affect significantly the stability contribution of tryptophans at different depths. However, because of the limited number of sites investigated, we do not exclude the possibility that membrane curvature may have more subtle effects on the contribution of aromatic residues to the folding of membrane proteins.

Contrary to all other lipid-contacting tryptophans in β1, Trp7 did not follow this general rule and had an unusually strong stabilization effect (p = 0.0002 statistical significance with $\Delta\Delta G^{\circ}_{Trp\text{-}Ala}$ values for W_7, W_9, W_{11}, W_{13}, and W_{15} mutants). This Trp is located in the periplasmic interface, where it potentially interacts with other nearby aromatic residues. W_7 was the most stable mutant among the mutants tested [$\Delta G^{\circ}_{unfold,H_2O}$ = 6.3 ± 0.5 kcal/mol (Figure 3C and Table 1)]. When compared to the comparable Trp15, which is located at the other membrane interface, Trp7 had an excess degree of stabilization of −2.6 ± 0.6 kcal/mol at 0 M urea (Figure 4). This particularly favorable contribution by Trp7 is most likely caused by its aromatic interaction with Tyr43 on β2. On the basis of the crystal structure of OmpA, the intercentroid distance between the aromatic cores of Trp7 and Tyr43 is 4.8 Å (Figure 1). We previously showed by double mutant cycle analysis that aromatic−aromatic interactions stabilize OmpA on the order of −1 to −2 kcal/mol ($\Delta\Delta G^{\circ}$) when the intercentroid distance between two neighboring aromatic

dx.doi.org/10.1021/bi400344b | Biochemistry 2013, 52, 4413−4421

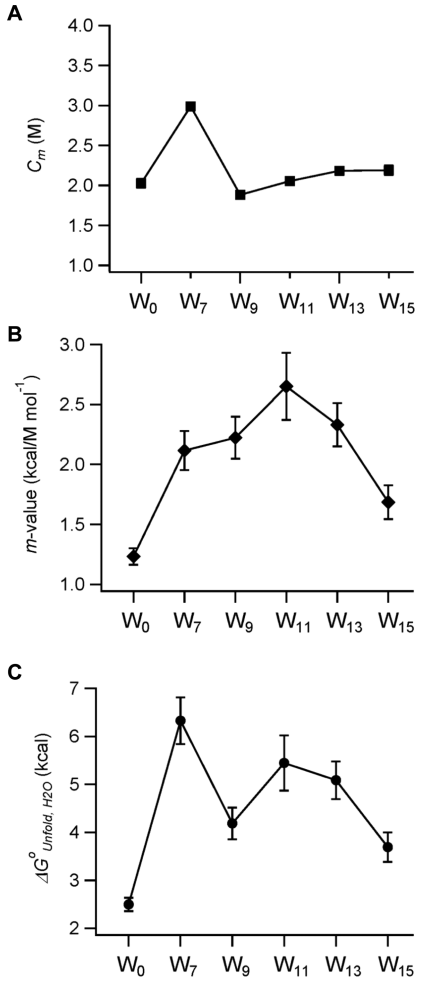

Figure 3. Plots of fitted parameters describing the equilibrium unfolding of OmpA depending on the position of the Trp residue along strand β1. (A) Midpoints of transition (C_m) and (B) *m*-values vs Trp position. (C) Free energy of unfolding ($\Delta G^{\circ}_{unfold,H_2O}$) depending on the position of the Trp residue.

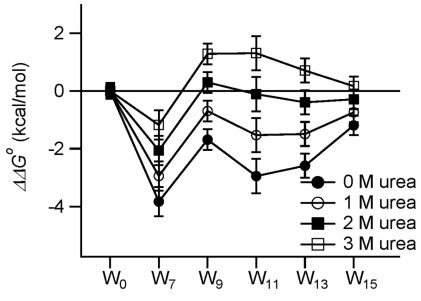

Figure 4. Difference free energies ($\Delta\Delta G^{\circ}_{Trp\text{-}Ala}$) vs Trp position for four urea concentrations. The values at 0 M urea are the customary $\Delta\Delta G^{\circ}_{unfold,H_2O}$ values.

rings is <7 Å.[22] The interaction energy between Trp7 and Tyr43 ($\Delta\Delta G^{\circ}$) is −1.0 kcal/mol.[22] Although the intercentroid distances between Trp7 and Tyr168 and between Trp7 and Phe170 are 8.3 and 13.4 Å, respectively, in the crystal structure (Figure 1), it is possible that Trp7 also favorably interacts with Tyr168 and/or Phe170 on β8 because these residues likely sample multiple conformations.[31] Although it is conceivable that Trp9 may also interact with the aromatic residues in β2 and β8, our results (Figures 3C and 4) do not indicate any interference by this potential interaction.

We were interested in knowing whether the energetic contributions of the different tryptophans depended on the folded reference state, i.e., whether different results would be obtained when $\Delta G^{\circ}_{unfold}$ was compared at a specific denaturant concentration (eq 4) rather than back-extrapolated to buffered water. Interestingly, the membrane depth-dependent contribution of Trp was highly sensitive to the concentration of urea (Figure 4). The most favorable contribution of the membrane-central Trp11 to the stability of OmpA gradually decreased as the urea concentration was increased and eventually was reversed at 3 M urea. However, the bell-shaped energy profile across the bilayer observed at 3 M urea may not be statistically significant (p = 0.037 with $\Delta\Delta G^{\circ}_{Trp\text{-}Ala}$ values for W_9, W_{11}, W_{13}, and W_{15} mutants) because of the relatively large standard errors compared to the small differences in $\Delta\Delta G^{\circ}_{Trp\text{-}Ala}$ values. However, the systematic trends observed as the urea concentration increases let us believe that the shape of the energy profile is indeed reversed when the high-urea reference states are compared with the low-urea reference states. At 3 M urea, which denatures OmpA significantly but not completely, the interfacial Trp15 appears to be more stabilizing than the central Trp11 by ∼1.1 ± 0.7 kcal/mol. All lipid-contacting tryptophans of β1 were moderately destabilizing at 3 M urea ($\Delta\Delta G^{\circ}_{Trp\text{-}Ala}[W_x] > 0$) (Figure 4). While the data at 0 M urea are clearly statistically significant, we are more cautious about the data observed at the higher urea concentrations. Regardless, we still find the observed systematic trends for folding in more destabilizing conditions interesting and perhaps biologically meaningful as we will further discuss below.

DISCUSSION

Aromatic residues play a unique role in protein−lipid interactions. On the basis of statistical analysis of membrane proteins of known structure, they are significantly enriched with Trp and Tyr in the water−bilayer interface, implying a crucial role of these residues in anchoring membrane proteins in lipid bilayers.[9−11,32] Their strong membrane-partitioning character is also important for the translocation of signaling and fusion proteins to lipid bilayers.[33−36] Physicochemical properties such as the aromaticity, electric quadrupole moment, and large hydrophobic surface area are thought to be responsible for these phenomena.[37] Among aromatic residues, Trp has a strong propensity to interact with phospholipids in the interfacial and hydrophobic core regions.[32]

Here, we systematically studied the effect of Trp placed at different depths in a lipid bilayer on the stability of β-barrel membrane protein OmpA. Lipid solvation of Trp stabilized OmpA at all depths but was most stabilizing when placed near the center of the bilayer. Stabilization by lipid solvation of Trp was gradually weakened as this residue was moved toward either membrane interface.

Our result that the central Trp is most stabilizing agrees with predictions from the Wimley−White (WW) whole-residue hydrophobicity scales.[4,5] While Trp is the most hydrophobic amino acid on both the water−octanol and water−interface scales, the partitioning of Trp into octanol that mimics the hydrocarbon region of the bilayer is more favorable than its partitioning into lipid bilayer interfaces. Indeed, the free energy differences between the two WW scales can be used to distinguish between helical segments of membrane proteins that span the lipid bilayer and those that partition to the

interface.[38] We can further use these scales to estimate the net preference of Trp for partitioning into the core of the bilayer relative to the bilayer interface according to

$$\Delta G^{\circ}_{\text{octanol-interface}}[\text{Trp-Ala}] = (\Delta G^{\circ}_{\text{water-octanol}}[\text{Trp}] - \Delta G^{\circ}_{\text{water-interface}}[\text{Trp}]) - (\Delta G^{\circ}_{\text{water-octanol}}[\text{Ala}] - \Delta G^{\circ}_{\text{water-interface}}[\text{Ala}]) \quad (5)$$

and we find $\Delta\Delta G^{\circ}_{\text{octanol-interface}}$ to equal -0.57 ± 0.18 kcal/mol, which implies a mild preference of Trp for the bilayer interior. For comparison, our result of the contribution of the interior tryptophans (W_9, W_{11}, and W_{13}) to the stability of OmpA in lipid bilayers relative to interfacial tryptophans (W_{15})

$$\Delta G^{\circ}_{\text{interior-interface}}[W_x] = (\Delta G^{\circ}_{\text{unfold}}[W_0] - \Delta G^{\circ}_{\text{unfold}}[W_x]) - (\Delta G^{\circ}_{\text{unfold}}[W_0] - \Delta G^{\circ}_{\text{unfold}}[W_{15}]) \quad (6)$$

where x = 9, 11, and 13, ranges from $\Delta\Delta G^{\circ}_{\text{interior-interface}} = -0.5 \pm 0.5$, -1.4 ± 0.5, and -1.8 ± 0.7 kcal/mol for W_9, W_{13}, and W_{11}, respectively. These values are on the same order of magnitude as or slightly greater than those estimated from the WW scales. In this comparison, we did not include W_7 because its true energetic contribution is masked by cooperative interaction with other aromatic residues in the neighboring strands[22,39] (see Results).

Contrary to the free energies derived from these membrane protein folding experiments and Wimley and White's peptide partitioning studies, recent work from the von Heijne group showed that the transfer of Trp from the translocon to the lipid bilayer of the ER is less favorable in the center than in both membrane interfaces by a $\Delta\Delta G^{\circ}_{\text{app}}$ of 0.8−1.0 kcal/mol.[7,40] Öjemalm et al. further tested various non-natural amino acid analogues of Trp, Tyr, and Phe and concluded that the hydrogen bonding capability of aromatic side chains is an important factor that determines the preference of polar aromatic residues for the interfaces over the interior of the ER membrane.[40] As already mentioned, many statistical analyses of the structures of α-helical and β-barrel membrane proteins also indicate a substantial enrichment of tryptophans at interfaces relative to the bilayer center,[9−11,32,41] although Adamian et al. find Trp similarly prevalent in the lipid hydrocarbon (ΔG = −0.3 kcal/mol) and headgroup (ΔG = −0.5 kcal/mol) regions.[32]

What could be the reasons for the apparent discrepancy between these different scales? The thermodynamic stability of proteins is defined as the free energy difference between the folded and unfolded states.[25] Therefore, the free energy of the unfolded state is also critically important for defining the thermodynamic stability of proteins, including membrane proteins. Could it be that we are seeing here a manifestation of different unfolded states in the *in vitro* biochemical and more biological cell-free systems? We think that this is actually quite likely. We know that OmpA has only negligible residual structure at 8 M urea.[20] Another β-barrel membrane protein of similar size, OmpX, also has only little residual structure at high denaturant concentrations.[42] The state of nascent proteins almost certainly is different from random coil in the translocon. Nascent proteins in the translocon channel are likely somehow ordered, although this order is of course very far from the native state of the protein and certainly different from the disorder found in an unfolded membrane protein in solution.

Even if no structure can be detected in intrinsically disordered proteins *in vitro*, they are not completely random either.[43] In addition to depth-dependent bilayer effects in the folded state, nonrandom unfolded states of our proteins could contribute to the depth-dependent folding profiles that we observed in this work. For example, it is conceivable that the central tryptophans (W_9, W_{11}, and W_{13} mutants) of OmpA destabilize the unfolded states more than the interfacial tryptophans (W_7 and W_{15} mutants). The notion that this may indeed be the case is supported by our observation that the Trp contribution to OmpA's stability was remarkably more sensitive to solvent perturbation by urea for tryptophans near the bilayer center than for interfacial tryptophans (Figure 4).

Another interesting observation is the large and systematic variation of the *m*-values of the mutants (Figure 3B). They are the principle players that drive the strong depth and urea dependence of the stability contribution of the different tryptophans in membranes (Figures 3B,C and 4). In soluble protein folding, *m*-values are generally believed to reflect how much hydrophobic surface area is shielded from water.[44,45] It is therefore not surprising that residues that are more deeply buried in the bilayer feature higher *m*-values. However, the nonrandomness of unfolded states also needs to be taken into account in discussions of the sequence dependence of *m*-values.[46] In this context, it is interesting to note that a Trp residue contributes to the formation of a single tiny cluster of local residual structure in the unfolded membrane protein OmpX in 8 M urea.[42]

Finally, the changes in the unfolding free energy by mutation of lipid-exposed residues are designed in our study to capture differential lipid−protein interactions of the replaced residues.[8,22] However, although we designed our experiments to minimize energetic interference from neighboring residues in the folded state, we cannot completely exclude the possibility that the apparent changes in the unfolding free energies are subject to subtle contributions from perturbed folded states of our OmpA mutants. However, such perturbations, if present, are likely only very minor as judged from the efficient refolding and spectroscopic characterization of all mutants. We also need to be cautious about the generality of our conclusions based on trends observed after mutation of just one strand of OmpA. Further mutational analysis, including deletion of the aromatic residues in neighboring strands β2 and β8 as well as targeting Trp residues in other β-strands, would be interesting to pursue.

In summary, our results suggest that lipid solvation of individual amino acid residues lining the membrane-embedded perimeter of integral membrane proteins is adjusted by the complex physicochemical properties of the lipid bilayer that vary dramatically with membrane depth. This fine-tuning affects quite strongly the thermodynamic stability of not only OmpA but most likely also all membrane proteins. For multipass α-helical or β-barrel membrane proteins, the depth-dependent lipid solvation is further modified by interactions with neighboring side chains in the native structure and likely also by energetic contributions from unfolded states.

■ ASSOCIATED CONTENT

Supporting Information

Detailed data fitting procedures for obtaining the unfolding free energy of OmpA and supplementary figures. This material is available free of charge via the Internet at http://pubs.acs.org.

dx.doi.org/10.1021/bi400344b | *Biochemistry* 2013, 52, 4413−4421

AUTHOR INFORMATION

Corresponding Author

*H.H.: e-mail, honghd@msu.edu; telephone, (517) 355-9715, ext. 352. L.K.T.: e-mail, lkt2e@virginia.edu; telephone, (434) 982-3578.

Funding

This work was supported by Grant R01 GM51329 from the National Institutes of Health (to L.K.T.) and start-up funds from Michigan State University (to H.H.).

Notes

The authors declare no competing financial interest.

ACKNOWLEDGMENTS

We thank Dr. Volker Kiessling at University of Virginia for providing the gel analysis program.

ABBREVIATIONS

DPoPC, 1, 2-dipalmitoleoyl-*sn*-glycero-3-phosphocholine; POPG, 1-palmitoyl-2-oleoyl-*sn*-glycero-3-[phospho(1-*rac*-glycerol)]; SUV, small unilamellar vesicle; SDS−PAGE, sodium dodecyl sulfate−polyacrylamide gel eletrophoresis; LB, Luria-Bertani medium.

REFERENCES

(1) White, S. H., and Wimley, W. C. (1999) Membrane protein folding and stability: Physical principles. *Annu. Rev. Biophys. Biomol. Struct. 28*, 319−365.

(2) Bowie, J. U. (2005) Solving the membrane protein folding problem. *Nature 438*, 581−589.

(3) Jayasinghe, S., Hristova, K., and White, S. H. (2001) Energetics, stability, and prediction of transmembrane helices. *J. Mol. Biol. 312*, 927−934.

(4) Wimley, W. C., Creamer, T. P., and White, S. H. (1996) Solvation energies of amino acid side chains and backbone in a family of host-guest pentapeptides. *Biochemistry 35*, 5109−5124.

(5) Wimley, W. C., and White, S. H. (1996) Experimentally determined hydrophobicity scale for proteins at membrane interfaces. *Nat. Struct. Biol. 3*, 842−848.

(6) Hessa, T., Kim, H., Bihlmaier, K., Lundin, C., Boekel, J., Andersson, H., Nilsson, I., White, S. H., and von Heijne, G. (2005) Recognition of transmembrane helices by the endoplasmic reticulum translocon. *Nature 433*, 377−381.

(7) Hessa, T., Meindl-Beinker, N. M., Bernsel, A., Kim, H., Sato, Y., Lerch-Bader, M., Nilsson, I., White, S. H., and von Heijne, G. (2007) Molecular code for transmembrane-helix recognition by the Sec61 translocon. *Nature 450*, 1026−1030.

(8) Moon, C. P., and Fleming, K. G. (2011) Side-chain hydrophobicity scale derived from transmembrane protein folding into lipid bilayers. *Proc. Natl. Acad. Sci. U.S.A. 108*, 10174−10177.

(9) Senes, A., Chadi, D. C., Law, P. B., Walters, R. F., Nanda, V., and Degrado, W. F. (2007) E(z), a depth-dependent potential for assessing the energies of insertion of amino acid side-chains into membranes: Derivation and applications to determining the orientation of transmembrane and interfacial helices. *J. Mol. Biol. 366*, 436−448.

(10) Schramm, C. A., Hannigan, B. T., Donald, J. E., Keasar, C., Saven, J. G., Degrado, W. F., and Samish, I. (2012) Knowledge-based potential for positioning membrane-associated structures and assessing residue-specific energetic contributions. *Structure 20*, 924−935.

(11) Ulmschneider, M. B., and Sansom, M. S. (2001) Amino acid distributions in integral membrane protein structures. *Biochim. Biophys. Acta 1512*, 1−14.

(12) de Planque, M. R., and Killian, J. A. (2003) Protein-lipid interactions studied with designed transmembrane peptides: Role of hydrophobic matching and interfacial anchoring. *Mol. Membr. Biol. 20*, 271−284.

(13) Killian, J. A., and von Heijne, G. (2000) How proteins adapt to a membrane-water interface. *Trends Biochem. Sci. 25*, 429−434.

(14) Landolt-Marticorena, C., Williams, K. A., Deber, C. M., and Reithmeier, R. A. (1993) Non-random distribution of amino acids in the transmembrane segments of human type I single span membrane proteins. *J. Mol. Biol. 229*, 602−608.

(15) Gleason, N. J., Vostrikov, V. V., Greathouse, D. V., Grant, C. V., Opella, S. J., and Koeppe, R. E., II (2012) Tyrosine replacing tryptophan as an anchor in GWALP peptides. *Biochemistry 51*, 2044−2053.

(16) Nozaki, Y., and Tanford, C. (1971) The solubility of amino acids and two glycine peptides in aqueous ethanol and dioxane solutions. Establishment of a hydrophobicity scale. *J. Biol. Chem. 246*, 2211−2217.

(17) Kyte, J., and Doolittle, R. F. (1982) A simple method for displaying the hydropathic character of a protein. *J. Mol. Biol. 157*, 105−132.

(18) Eisenberg, D., Weiss, R. M., and Terwilliger, T. C. (1982) The helical hydrophobic moment: A measure of the amphiphilicity of a helix. *Nature 299*, 371−374.

(19) Engelman, D. M., Steitz, T. A., and Goldman, A. (1986) Identifying nonpolar transbilayer helices in amino acid sequences of membrane proteins. *Annu. Rev. Biophys. Biophys. Chem. 15*, 321−353.

(20) Hong, H., and Tamm, L. K. (2004) Elastic coupling of integral membrane protein stability to lipid bilayer forces. *Proc. Natl. Acad. Sci. U.S.A. 101*, 4065−4070.

(21) Huysmans, G. H., Baldwin, S. A., Brockwell, D. J., and Radford, S. E. (2010) The transition state for folding of an outer membrane protein. *Proc. Natl. Acad. Sci. U.S.A. 107*, 4099−4104.

(22) Hong, H., Park, S., Jimenez, R. H., Rinehart, D., and Tamm, L. K. (2007) Role of aromatic side chains in the folding and thermodynamic stability of integral membrane proteins. *J. Am. Chem. Soc. 129*, 8320−8327.

(23) Kleinschmidt, J. H., den Blaauwen, T., Driessen, A. J., and Tamm, L. K. (1999) Outer membrane protein A of *Escherichia coli* inserts and folds into lipid bilayers by a concerted mechanism. *Biochemistry 38*, 5006−5016.

(24) Prilipov, A., Phale, P. S., Van Gelder, P., Rosenbusch, J. P., and Koebnik, R. (1998) Coupling site-directed mutagenesis with high-level expression: Large scale production of mutant porins from *E. coli*. *FEMS Microbiol. Lett. 163*, 65−72.

(25) Fersht, A. R., Matouschek, A., and Serrano, L. (1992) The folding of an enzyme. I. Theory of protein engineering analysis of stability and pathway of protein folding. *J. Mol. Biol. 224*, 771−782.

(26) Kirkman, T. W. (1996) Statistics to use. http://www.physics.csbsju.edu/stats/ (accessed March 5, 2013).

(27) Pautsch, A., and Schulz, G. E. (2000) High-resolution structure of the OmpA membrane domain. *J. Mol. Biol. 298*, 273−282.

(28) Tusnady, G. E., Dosztanyi, Z., and Simon, I. (2005) PDB_TM: Selection and membrane localization of transmembrane proteins in the Protein Data Bank. *Nucleic Acids Res. 33*, D275−D278.

(29) Rodionova, N. A., Tatulian, S. A., Surrey, T., Jahnig, F., and Tamm, L. K. (1995) Characterization of two membrane-bound forms of OmpA. *Biochemistry 34*, 1921−1929.

(30) Kleinschmidt, J. H., and Tamm, L. K. (1996) Folding intermediates of a β-barrel membrane protein. Kinetic evidence for a multi-step membrane insertion mechanism. *Biochemistry 35*, 12993−13000.

(31) Liang, B., Arora, A., and Tamm, L. K. (2010) Fast-time scale dynamics of outer membrane protein A by extended model-free analysis of NMR relaxation data. *Biochim. Biophys. Acta 1798*, 68−76.

(32) Adamian, L., Nanda, V., DeGrado, W. F., and Liang, J. (2005) Empirical lipid propensities of amino acid residues in multispan α helical membrane proteins. *Proteins 59*, 496−509.

(33) Lai, A. L., Park, H., White, J. M., and Tamm, L. K. (2006) Fusion peptide of influenza hemagglutinin requires a fixed angle boomerang structure for activity. *J. Biol. Chem. 281*, 5760−5770.

(34) Ellena, J. F., Liang, B. Y., Wiktor, M., Stein, A., Cafiso, D. S., Jahn, R., and Tamm, L. K. (2009) Dynamic structure of lipid-bound

synaptobrevin suggests a nucleation-propagation mechanism for trans-SNARE complex formation. *Proc. Natl. Acad. Sci. U.S.A. 106*, 20306−20311.
(35) Popa, A., Pager, C. T., and Dutch, R. E. (2011) C-Terminal Tyrosine Residues Modulate the Fusion Activity of the Hendra Virus Fusion Protein. *Biochemistry 50*, 945−952.
(36) Cho, W. H., and Stahelin, R. V. (2005) Membrane-protein interactions in cell signaling and membrane trafficking. *Annu. Rev. Biophys. Biomol. Struct. 34*, 119−151.
(37) Yau, W. M., Wimley, W. C., Gawrisch, K., and White, S. H. (1998) The preference of tryptophan for membrane interfaces. *Biochemistry 37*, 14713−14718.
(38) Snider, C., Jayasinghe, S., Hristova, K., and White, S. H. (2009) MPEx: A tool for exploring membrane proteins. *Protein Sci. 18*, 2624−2628.
(39) Sanchez, K. M., Gable, J. E., Schlamadinger, D. E., and Kim, J. E. (2008) Effects of tryptophan microenvironment, soluble domain, and vesicle size on the thermodynamics of membrane protein folding: Lessons from the transmembrane protein OmpA. *Biochemistry 47*, 12844−12852.
(40) Ojemalm, K., Higuchi, T., Jiang, Y., Langel, U., Nilsson, I., White, S. H., Suga, H., and von Heijne, G. (2011) Apolar surface area determines the efficiency of translocon-mediated membrane-protein integration into the endoplasmic reticulum. *Proc. Natl. Acad. Sci. U.S.A. 108*, E359−E364.
(41) Wimley, W. C. (2002) Toward genomic identification of β-barrel membrane proteins: Composition and architecture of known structures. *Protein Sci. 11*, 301−312.
(42) Tafer, H., Hiller, S., Hilty, C., Fernandez, C., and Wuthrich, K. (2004) Nonrandom structure in the urea-unfolded *Escherichia coli* outer membrane protein X (OmpX). *Biochemistry 43*, 860−869.
(43) Uversky, V. N. (2002) Natively unfolded proteins: A point where biology waits for physics. *Protein Sci. 11*, 739−756.
(44) Shortle, D. (1995) Staphylococcal Nuclease: A Showcase of M-Value Effects. *Adv. Protein Chem. 46*, 217−247.
(45) Shortle, D., Chan, H. S., and Dill, K. A. (1992) Modeling the effects of mutations on the denatured states of proteins. *Protein Sci. 1*, 201−215.
(46) Dill, K. A., and Shortle, D. (1991) Denatured states of proteins. *Annu. Rev. Biochem. 60*, 795−825.